Anomalous Absorption by the Two-Plasmon Decay Instability

D. Turnbull,* A. V. Maximov, D. H. Edgell, W. Seka, R. K. Follett, J. P. Palastro, D. Cao,
V. N. Goncharov, C. Stoeckl, and D. H. Froula
University of Rochester Laboratory for Laser Energetics, 250 E River Road, Rochester, New York 14623, USA

(Received 18 October 2019; revised manuscript received 11 March 2020; accepted 17 April 2020; published 5 May 2020)

Radiation-hydrodynamic simulations of directly driven fusion experiments at the Omega Laser Facility predict absorption accurately when targets are driven at low overlapped laser intensity. Discrepancies appear at increased intensity, however, with higher-than-expected laser absorption on target. Strong correlations with signatures of the two-plasmon decay (TPD) instability—including half-harmonic and hard-x-ray emission—indicate that TPD is responsible for this anomalous absorption. Scattered light data suggest that up to ≈30% of the laser power reaching quarter-critical density can be absorbed locally when the TPD threshold is exceeded. A scaling of absorption versus TPD threshold parameter was empirically determined and validated using the laser–plasma simulation environment code.

DOI: 10.1103/PhysRevLett.124.185001

In direct-drive inertial confinement fusion (ICF), an ensemble of laser beams uniformly illuminates a spherical shell, ablating the outer layer in order to accelerate a deuterium-tritium ice layer inward via the rocket effect [1,2]. When the fuel stagnates, the conversion of kinetic to thermal energy rapidly increases its temperature to a level where fusion reactions occur. The coupling of the drive laser to the target is arguably the most fundamental ingredient of such implosions, necessitating accurate models that capture all of the primary laser absorption processes.

In radiation-hydrodynamic simulations (i.e., using the LILAC code [3]), the recent transition from a flux-limited thermal transport model to a more physical nonlocal model [4] revealed significant errors in predicted laser absorption, with more light scattered from the target than expected. This led to the realization that resonant amplification of unabsorbed light leaving the target (i.e., crossed-beam energy transfer, or CBET) significantly degrades the laser coupling. Simulation fidelity was improved [5,6] by the addition of an inline model describing the instability [7].

This model, however, ostensibly overcompensates—increasing scattered light and reducing shell velocity beyond the level suggested by measurements. Since laser-plasma instabilities have historically been difficult to predict quantitatively, this discrepancy was attributed to errors in CBET modeling, and an *ad hoc* tuning multiplier was added in order to better match the data [7,8]. Recent parallel efforts to conduct isolated CBET experiments under well-characterized conditions suggest, however, that the linear inline CBET models should be accurate in the relevant parameter space [9,10].

Another laser-plasma instability of critical importance in OMEGA-scale direct-drive implosions is the two-plasmon decay (TPD) instability [11–13], in which an incident photon decays into two electron plasma waves near the quarter-critical density surface, $n_c/4$. Previous work was primarily concerned with its tendency to generate a suprathermal electron population that can degrade implosion performance by preheating the fuel and reducing compressibility [14–19]. Naively, since the fractional laser energy into hot electrons tends to saturate at the 1% level [20,21], one might expect the impact of TPD on overall energetics to be negligible; however, if collisional damping is dominant over Landau damping, the driven plasma waves primarily heat the local thermal population rather than produce suprathermal electrons [22,23].

In this Letter, we show that the discrepancy between predicted and observed scattered light is a signature of anomalous absorption of laser light due to the excitation of TPD. Over a wide range of laser intensities spanning the typical design space of implosions on OMEGA, the time-dependent absorption difference is shown to be strongly correlated with the time history of TPD activity, which was diagnosed using half-harmonic emission. Furthermore, the time-integrated difference in total scattered energy scales with hard x-ray emission—another observable that is known to track TPD [14,15,20]. The data suggest that ≈15% to 20% of the laser light reaching $n_c/4$ is typically absorbed when TPD is active, which significantly modifies the coronal plasma energetics of implosions on OMEGA.

An illustration of the 1D power balance is shown in Fig. 1. The incident lasers transfer energy to the coronal plasma through electron-ion collisions. Between approximately $0.1n_c$ to $0.5n_c$, the incident light is also coupled to the outgoing light by CBET. When the ingoing rays reach their turning point, the photons that have not yet been absorbed get reflected. Upon reentering the CBET-active region, this outgoing light becomes the seed that is amplified by CBET. The solid and dashed black lines

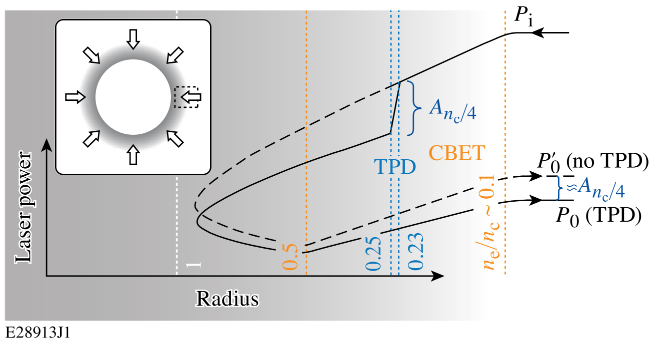

FIG. 1. Illustration of laser power balance in the coronal plasma of a direct-drive implosion, with (solid curve) and without (dashed curve) the excitation of TPD. With TPD, scattered power out is reduced by approximately the fraction of the light reaching $n_c/4$ that gets absorbed locally.

qualitatively illustrate the laser power trajectories with and without TPD, respectively. When some fraction of the incident laser light is absorbed near $n_c/4$ due to TPD, the power at every point thereafter will be reduced by approximately that fraction, including the net power out.

Figure 2(a) shows the total incident laser power for six different implosions along with the scattered light predicted by LILAC (using the nonlocal and CBET models) and the measured scattered light. The experimental measurement averages the streaked spectrometer traces from the two absolutely calibrated full-aperture backscatter (FABS) stations as well as the two cross-calibrated sidescatter ports [24]. The time-dependent error bar is the maximum of either $\pm 1.5\%$ of the instantaneous laser power (based on the standard deviation of the typical time-integrated coupling difference suggested by the two independent FABS measurements) or the instantaneous standard deviation of the four signals. For completeness, the time-integrated coupling percentage (incident energy minus scattered energy, all divided by incident energy) is also included for both the simulations and the experiments, with differences as large as 8% (shot 76824). For these experiments, target diameters ranged from 805 μm to 914 μm, and standard laser smoothing was employed [i.e., either "SG4" (704-μm FWHM) or "SG5" (714-μm FWHM) phase plates, where the nomenclature refers to the super-Gaussian exponent of the far-field spatial profile; smoothing by spectral dispersion; and polarization smoothing].

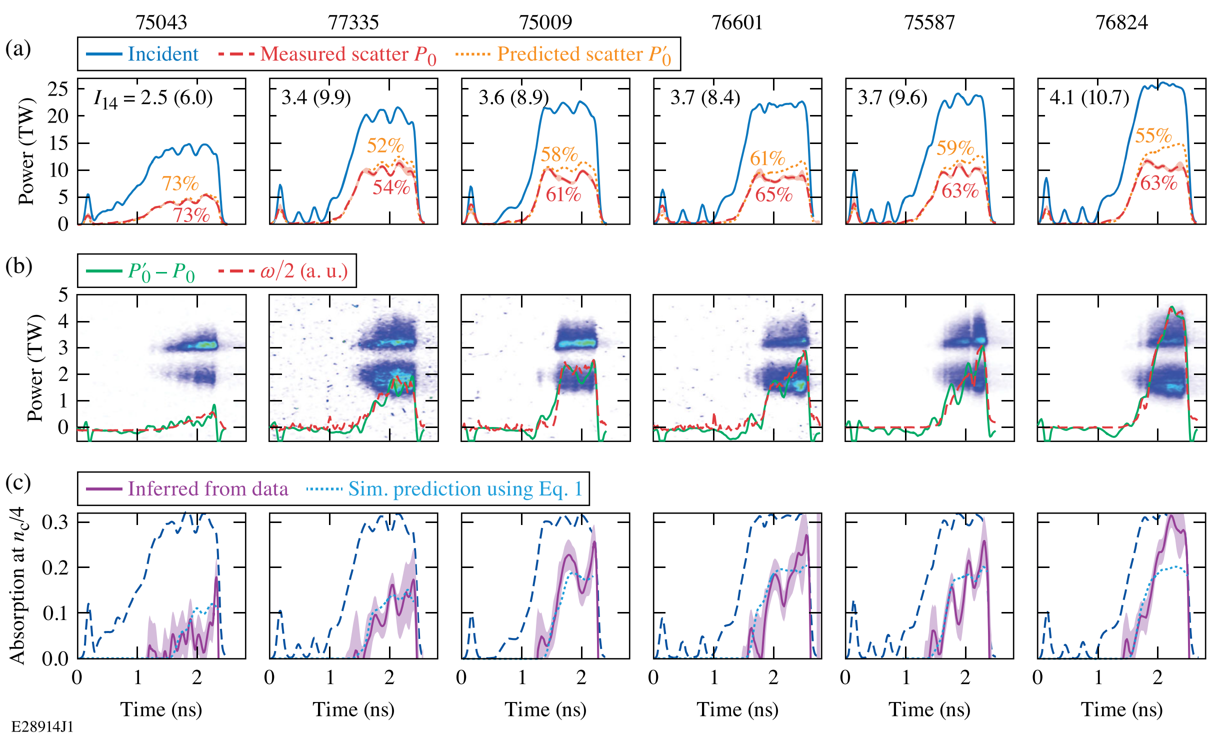

FIG. 2. Use of scattered light data to infer anomalous absorption due to TPD. (a) From left to right, peak power increases along with overlapped intensity at quarter-critical density (labeled I_{14} in units of 10^{14} W/cm^2), although vacuum hard-sphere intensities (provided parenthetically) are somewhat decoupled due to initial target size variation. During peak power, scattered light data are increasingly divergent from the simulated predictions as quarter-critical intensity increases. (b) The difference between predicted and observed scattered light correlates extremely well with half-harmonic emission, indicating the discrepancy is associated with TPD. (c) Assuming that anomalous absorption by TPD primarily reduces the unabsorbed light seed for CBET, absorption at $n_c/4$ due to TPD is typically found to be in the range of $\approx$10% to 25%. The absorption time dependence can be predicted inline using parameters in LILAC along with Eq. (1) and the response function described in the text.

Figure 2(a) also lists the average quarter-critical overlapped intensity during the peak according to LILAC (ranging from $I_{14} = 2.5$ to 4.1 in units of $10^{14}\ \mathrm{W/cm^2}$) and the associated vacuum hard-sphere intensities (6.0 to 10.7).

The examples shown are emblematic of the systematic trends evident in the broader absorption database. At low overlapped intensity (e.g., shot 75043), there is excellent agreement between predicted and observed scattered light. At higher quarter-critical intensity, however, they tend to diverge at some point during peak power. Several notable trends suggested possible connection to the TPD instability: (1) the sometimes abrupt onset of the discrepancy (cf. 75009 and 76601); (2) the tendency for the discrepancy to grow during peak power (cf. 77335 and 75587); and (3) the overall trend of worsening agreement with increased intensity.

In search of qualitative correlation between the apparent error in scattered light and TPD, the time-resolved difference between the predicted and observed scattered light was plotted against the time history of half-harmonic ($\omega/2$) emission—a spectral doublet centered around 702 nm that is known to be a signature of TPD [11]. The results are shown in Fig. 2(b). The agreement in terms of onset, timing, and overall shape is particularly remarkable for shots 76601 and 76824, although general trends are consistent for all shots. Because of the nonlinear, threshold nature of TPD, minor changes in pulse shape and target type result in unique and dynamic time histories of TPD activity on each shot; nevertheless, the absorption discrepancy tends to track detailed features very closely. Note also that from the perspective of most processes (i.e., heat transport, or CBET), coronal plasma conditions evolve slowly during peak power. Only TPD evolves rapidly once its threshold is exceeded, so the associated rapid changes in absorption are most likely caused by TPD. On shots 75587 and 76824, an additional streaked spectrometer measured $3\omega/2$ emission, yielding normalized time histories nearly identical to the $\omega/2$ emission (as previously observed [11]). This is likely due to the instability reaching the nonlinear saturation stage in which a broad spectrum of electron plasma waves is excited, and it indicates that each signature is broadly representative of the overall TPD time history.

However, the streaked spectrometer used to record the $\omega/2$ emission is not maintained as an absolutely calibrated diagnostic. To more quantitatively assess the correlation between the absorption difference and TPD, the difference curves were integrated to give the total error in scattered energy, which was then plotted (cf. Fig. 3) against the total signal from hard x rays with energy > 40 keV measured by the hard x-ray detector (HXRD) [14,15]. The 16 points represent shots that took place between 2014 and 2015, a subset of which is highlighted in cyan because they coincide with those featured in Fig. 1. The leftmost featured point is shot 75043, where there was little apparent error in scattered light as well as a very small hard x-ray signal

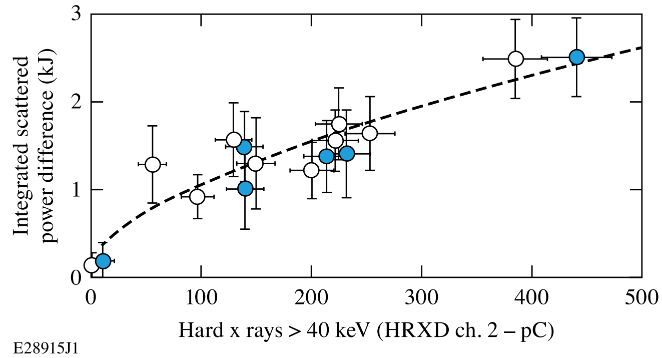

FIG. 3. The total integrated scattered power difference on a wide variety of shots correlates with the measurement of hard x rays > 40 keV from HXRD channel 2, confirming that the discrepancies in scattered light are related to TPD.

(which indicates few hot electrons and minimal TPD activity). At the other extreme, shot 76824 had the largest scattered energy difference (exceeding 2.5 kJ) as well as the highest hard x-ray signal. Overall, the trend is clear and bolsters the case for a causal relationship between TPD and the scattered light reduction.

Assuming the decrease in total scattered power is dominated by the reduction of the unabsorbed light seed (as illustrated in Fig. 1), the ratio of scattered power with TPD (i.e., the experimental result) to scattered power without TPD (i.e., the simulated result) is a direct measurement of the transmission T past $n_c/4$, and absorption is simply $A_{n_c/4} = 1 - T$ [Fig. 2(c)]. The normalized pulse shape is included on each subplot to retain a sense of the timing, with TPD activity tending to occur during the latter $\approx 2/3$ of peak power. Typical incident power levels yield absorption in the range of 10% to 25%. Such levels are consistent with the conclusions drawn from electron temperature measurements of the quarter-critical region based on half-harmonic emission [25].

It would be useful to have an inline model for enhanced TPD absorption that does not rely on experimental measurements *a posteriori*; inferring an appropriate scaling for such a reduced model is a main goal of this work. TPD activity has previously been shown to scale with the Simon threshold parameter $\eta = I_{14}L/(233T_e)$, with the density gradient scale length L in μm, electron temperature T_e in keV, and laser intensity specified at $n_c/4$ [11,16,19,26–28]. Strictly speaking, the Simon threshold refers to the absolute instability threshold for a single plane-wave beam, but it has been shown that substituting overlapped intensity for single-beam intensity still yields a threshold close to 1 for OMEGA's spherical illumination geometry and standard laser smoothing [11,19,28].

For each of the shots represented in Fig. 3, $\eta(t)$ was extracted from the LILAC simulations and plotted against the inferred absorption. While it was clear that TPD activity tracked the threshold parameter, there was an apparent lag

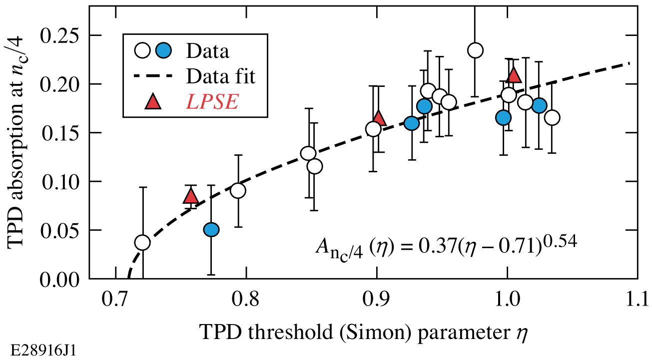

FIG. 4. A trend of inferred absorption versus the Simon threshold parameter extracted from simulations is found using the average values from a wide range of shots with differing drive conditions. Typically, conditions during peak power are ≈20% to 30% above the TPD threshold, resulting in ≈15% to 20% local absorption at $n_c/4$. Two-dimensional LPSE simulations accurately reproduce both the threshold and the scaling above threshold.

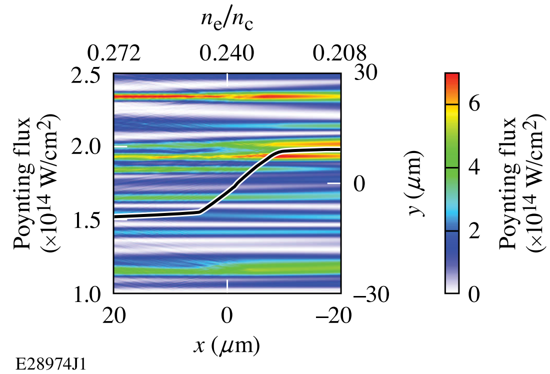

FIG. 5. Example of the LPSE simulation results. For $\eta \approx 1$ at time $t = 20$ ps, ≈22% absorption occurring over a narrow ≈10 μm-wide region was observed. Only a few intense speckles dominate the overall instability.

in the TPD response. To account for this delay and determine the most accurate scaling, the average absorption over the approximate duration of TPD activity was compared to average η over the same length of time but shifted 150 ps earlier. Figure 4 shows the inferred scaling of anomalous TPD absorption versus TPD threshold parameter. The best fit to the data in the form $a(x-b)^n$ gives

$$A_{n_c/4} = 0.37(\eta - 0.71)^{0.54} \tag{1}$$

above a threshold of $\eta = 0.71$. The 95% confidence bounds (a[0.22,0.52]; b[0.67,0.75]; and n[0.22,0.86]) suggest the threshold is well constrained although the shape of the curve is less well constrained given the scatter and limited range of the data.

Convolving the simulated Simon threshold parameter with an appropriate response function (determined to be a 120-ps–FWHM Gaussian with a 150-ps delay) and then applying the above scaling yields estimated absorption using the code parameters for direct comparison to the data on an individual shot. The results, included in Fig. 2(c), generally track the data well. This should therefore be a good starting point for a reduced model that can be included inline in radiation-hydrodynamic simulations.

We recognize that there will be several feedback mechanisms we have thus far neglected. For example, it has been shown that TPD activity elevates the thermal temperature around $n_c/4$ [25], which will reduce CBET in at least that location through the $1/T_e$ gain dependence. A previous attempt to include feedback on the hydrodynamic plasma conditions, however, observed a very modest increase in temperature [29]. Inside $n_c/4$, CBET gain will also be reduced by the lower "pump" power. On the other hand, less scattered power implies less overall energy transfer due to CBET and therefore less pump depletion, which will *increase* the pump power outside $n_c/4$. Since several of these effects are offsetting and none can seemingly grow large until absorption is significant, they are neglected here. Once a reduced model has been incorporated into the simulations, however, these additional effects will be taken into account self-consistently.

To validate the empirical scaling, 2D simulations were run using the laser-plasma simulation environment (LPSE) code [30], which has been shown previously to agree well with TPD experiments [31,32]. LPSE is a wave-based code with a fluid plasma response and a module that solves the extended Zakharov equations of TPD to simulate the coupling between electromagnetic waves, electron plasma waves, and ion acoustic waves. Notably, a new pump-depletion model was used that self-consistently evolves the electromagnetic field of the laser as power is pumped into electron plasma waves. To mimic OMEGA-scale implosion conditions, the following parameters were used: $L = 150$ μm, $T_e = 2.5$ keV, $T_i/T_e = 0.5$, and $Z = 3.5$. The simulations used a single speckled beam with in-plane polarization, and laser intensity was varied to span a range of η relevant to the experiments. [Note that the intensity (and therefore η) used in simulations was doubled in the ensuing discussion and Fig. 4 for a more direct comparison to experiments, which used polarization smoothing. Note also that these simulations omitted stimulated Raman scattering (SRS), and in some cases SRS and TPD can merge into a more complex "high-frequency hybrid instability," [33,34] although it is believed that the half-harmonic spectra justify this omission.] An example of the results is shown in Fig. 5 for $\eta \approx 1$ at time $t = 20$ ps giving ≈22% absorption.

Figure 4 shows that LPSE's predictions for TPD absorption are in very good agreement with the data. Each point is an ensemble average over a number of runs (20 near threshold and 4 otherwise), with absorption averaged over the period between 30 and 50 ps (well after most runs had reached steady state). The use of a speckled beam was found to be essential in reproducing both the threshold and the scaling above threshold because individual intense speckles go unstable below $\eta = 1$, while other parts of the beam remain below threshold. The simulations did produce a broad spectrum of electron plasma waves extending out to the Landau cutoff in the nonlinear saturation stage—consistent with the agreement between the $\omega/2$ and $3\omega/2$ emission that was noted earlier. Note that the only mechanism by which TPD depletes laser power in LPSE is through the damping of electron plasma waves driven up by the incident light. Critically, the simulations found that $5\times$ to $8.3\times$ more power is dissipated by collisional (rather than Landau) damping, which explains why such large laser absorption does not result in undue levels of hot electrons—most of the power is thermalized around $n_c/4$.

The implications of this effect on 1D implosion energetics are fairly clear. Overall absorption is enhanced but deposition is redistributed, with more plasma heating at lower density where the energy couples less efficiently to the ablation surface. The impact on shell trajectories will be investigated in the future. Multidimensional effects are also possible and likely more concerning. It is well known that TPD activity is sensitive to details such as polarization orientation and illumination symmetry [12,35]. On OMEGA, this causes preferential excitation at pent and hex centers (where there is 5- and 6-beam illumination symmetry, respectively) [25,28]. If TPD is driven nonuniformly around the target surface and is also associated with significant laser absorption, it might introduce substantial drive asymmetries (in particular, an $l = 10$ mid-mode seems likely [36]) that could confound recent efforts to achieve 1% power balance of the incident laser beams on target.

This material is based upon work supported by the Department of Energy National Nuclear Security Administration under Award No. DE-NA0003856, the University of Rochester, and the New York State Energy Research and Development Authority. This report was prepared as an account of work sponsored by an agency of the U.S. Government. Neither the U.S. Government nor any agency thereof, nor any of their employees, makes any warranty, express or implied, or assumes any legal liability or responsibility for the accuracy, completeness, or usefulness of any information, apparatus, product, or process disclosed, or represents that its use would not infringe privately owned rights. The views and opinions of authors expressed herein do not necessarily state or reflect those of the U.S. Government or any agency thereof.

*turnbull@lle.rochester.edu

[1] R. S. Craxton *et al.*, Phys. Plasmas **22**, 110501 (2015).
[2] E. Campbell *et al.*, Matter Radiat. Extremes **2**, 37 (2017).
[3] J. Delettrez, R. Epstein, M. C. Richardson, P. A. Jaanimagi, and B. L. Henke, Phys. Rev. A **36**, 3926 (1987).
[4] V. N. Goncharov, O. V. Gotchev, E. Vianello, T. R. Boehly, J. P. Knauer, P. W. McKenty, P. B. Radha, S. P. Regan, T. C. Sangster, S. Skupsky, V. A. Smalyuk, R. Betti, R. L. McCrory, D. D. Meyerhofer, and C. Cherfils-Clerouin, Phys. Plasmas **13**, 012702 (2006).
[5] V. N. Goncharov *et al.*, Phys. Plasmas **21**, 056315 (2014).
[6] P. B. Radha *et al.*, Phys. Plasmas **23**, 056305 (2016).
[7] I. V. Igumenshchev, D. H. Edgell, V. N. Goncharov, J. A. Delettrez, A. V. Maximov, J. F. Myatt, W. Seka, A. Shvydky, S. Skupsky, and C. Stoeckl, Phys. Plasmas **17**, 122708 (2010).
[8] I. V. Igumenshchev *et al.*, Phys. Plasmas **19**, 056314 (2012).
[9] D. Turnbull, C. Goyon, G. E. Kemp, B. B. Pollock, D. Mariscal, L. Divol, J. S. Ross, S. Patankar, J. D. Moody, and P. Michel, Phys. Rev. Lett. **118**, 015001 (2017).
[10] D. Turnbull, A. Colaïtis, R. K. Follett, J. P. Palastro, D. H. Froula, P. Michel, C. Goyon, T. Chapman, L. Divol, G. E. Kemp, D. Mariscal, S. Patankar, B. B. Pollock, J. S. Ross, J. D. Moody, E. R. Tubman, and N. C. Woolsey, Plasma Phys. Controlled Fusion **60**, 054017 (2018).
[11] W. Seka, D. H. Edgell, J. F. Myatt, A. V. Maximov, R. W. Short, V. N. Goncharov, and H. A. Baldis, Phys. Plasmas **16**, 052701 (2009).
[12] J. Zhang, J. F. Myatt, R. W. Short, A. V. Maximov, H. X. Vu, D. F. DuBois, and D. A. Russell, Phys. Rev. Lett. **113**, 105001 (2014).
[13] R. K. Follett, J. A. Delettrez, D. H. Edgell, V. N. Goncharov, R. J. Henchen, J. Katz, D. T. Michel, J. F. Myatt, J. Shaw, A. A. Solodov, C. Stoeckl, B. Yaakobi, and D. H. Froula, Phys. Rev. Lett. **116**, 155002 (2016).
[14] B. Yaakobi, C. Stoeckl, W. Seka, J. A. Delettrez, T. C. Sangster, and D. D. Meyerhofer, Phys. Plasmas **12**, 062703 (2005).
[15] V. A. Smalyuk, D. Shvarts, R. Betti, J. A. Delettrez, D. H. Edgell, V. Y. Glebov, V. N. Goncharov, R. L. McCrory, D. D. Meyerhofer, P. B. Radha, S. P. Regan, T. C. Sangster, W. Seka, S. Skupsky, C. Stoeckl, B. Yaakobi, J. A. Frenje, C. K. Li, R. D. Petrasso, and F. H. Séguin, Phys. Rev. Lett. **100**, 185005 (2008).
[16] H. X. Vu, D. F. DuBois, J. F. Myatt, and D. A. Russell, Phys. Plasmas **19**, 102703 (2012).
[17] J. F. Myatt, J. Zhang, J. A. Delettrez, A. V. Maximov, R. W. Short, W. Seka, D. H. Edgell, D. F. DuBois, D. A. Russell, and H. X. Vu, Phys. Plasmas **19**, 022707 (2012).
[18] B. Yaakobi, A. A. Solodov, J. F. Myatt, J. A. Delettrez, C. Stoeckl, and D. H. Froula, Phys. Plasmas **20**, 092706 (2013).
[19] J. A. Delettrez, T. J. B. Collins, and C. Ye, Phys. Plasmas **26**, 062705 (2019).
[20] C. Stoeckl, R. E. Bahr, B. Yaakobi, W. Seka, S. P. Regan, R. S. Craxton, J. A. Delettrez, R. W. Short, J. Myatt, A. V. Maximov, and H. Baldis, Phys. Rev. Lett. **90**, 235002 (2003).
[21] D. H. Froula, B. Yaakobi, S. X. Hu, P.-Y. Chang, R. S. Craxton, D. H. Edgell, R. Follett, D. T. Michel, J. F. Myatt, W. Seka, R. W. Short, A. Solodov, and C. Stoeckl, Phys. Rev. Lett. **108**, 165003 (2012).

[22] R. Yan, C. Ren, J. Li, A. V. Maximov, W. B. Mori, Z.-M. Sheng, and F. S. Tsung, Phys. Rev. Lett. **108**, 175002 (2012).
[23] J. F. Myatt, H. X. Vu, D. F. DuBois, D. A. Russell, J. Zhang, R. W. Short, and A. V. Maximov, Phys. Plasmas **20**, 052705 (2013).
[24] W. Seka, D. H. Edgell, J. P. Knauer, J. F. Myatt, A. V. Maximov, R. W. Short, T. C. Sangster, C. Stoeckl, R. E. Bahr, R. S. Craxton, J. A. Delettrez, V. N. Goncharov, I. V. Igumenshchev, and D. Shvarts, Phys. Plasmas **15**, 056312 (2008).
[25] W. Seka, J. F. Myatt, R. W. Short, D. H. Froula, J. Katz, V. N. Goncharov, and I. V. Igumenshchev, Phys. Rev. Lett. **112**, 145001 (2014).
[26] C. S. Liu and M. N. Rosenbluth, Phys. Fluids **19**, 967 (1976).
[27] A. Simon, R. W. Short, E. A. Williams, and T. Dewandre, Phys. Fluids **26**, 3107 (1983).
[28] J. F. Myatt, J. Shaw, V. N. Goncharov, J. Zhang, A. V. Maximov, R. W. Short, R. K. Follett, W. Seka, D. H. Edgell, and D. H. Froula, J. Phys. Conf. Ser. **717**, 012040 (2016).
[29] J. Li, S. X. Hu, and C. Ren, Phys. Plasmas **24**, 022706 (2017).
[30] J. F. Myatt, J. G. Shaw, R. K. Follett, D. H. Edgell, D. H. Froula, J. P. Palastro, and V. N. Goncharov, J. Comput. Phys. **399**, 108916 (2019).
[31] R. K. Follett, D. H. Edgell, R. J. Henchen, S. X. Hu, J. Katz, D. T. Michel, J. F. Myatt, J. Shaw, and D. H. Froula, Phys. Rev. E **91**, 031104(R) (2015).
[32] R. K. Follett, J. F. Myatt, J. G. Shaw, D. T. Michel, A. A. Solodov, D. H. Edgell, B. Yaakobi, and D. H. Froula, Phys. Plasmas **24**, 102134 (2017).
[33] B. B. Afeyan and E. A. Williams, Phys. Rev. Lett. **75**, 4218 (1995).
[34] B. B. Afeyan and E. A. Williams, Phys. Plasmas **4**, 3845 (1997).
[35] D. T. Michel, A. V. Maximov, R. W. Short, J. A. Delettrez, D. Edgell, S. X. Hu, I. V. Igumenshchev, J. F. Myatt, A. A. Solodov, C. Stoeckl, B. Yaakobi, and D. H. Froula, Phys. Plasmas **20**, 055703 (2013).
[36] A. Bose *et al.*, Phys. Plasmas **25**, 062701 (2018).